Title

Molecular targeting of papillary thyroid carcinoma with fluorescently labeled ratiometric activatable cell penetrating peptides in a transgenic murine model

Journal

Journal of Surgical Oncology, 113(2)

ISSN

8756-0437

Authors

Orosco, Ryan K
Savariar, Elamprakash N
Weissbrod, Philip A
et al.

Publication Date

2016-02-01

DOI

10.1002/jso.24129

Peer reviewed

HHS Public Access

Author manuscript

J Surg Oncol. Author manuscript; available in PMC 2017 February 01.

Published in final edited form as:

J Surg Oncol. 2016 February ; 113(2): 138–143. doi:10.1002/jso.24129.

Molecular Targeting of Papillary Thyroid Carcinoma With Fluorescently Labeled Ratiometric Activatable Cell Penetrating Peptides in a Transgenic Murine Model

RYAN K. OROSCO, MD[1], **ELAMPRAKASH N. SAVARIAR, PhD**[2], **PHILIP A. WEISSBROD, MD**[1], **JULIO A. DIAZ-PEREZ, MD**[3], **MICHAEL BOUVET, MD**[4], **ROGER Y. TSIEN, PhD**[2,5], and **QUYEN T. NGUYEN, MD, PhD**[1,*]

[1]Department of Surgery, Division of Head and Neck Surgery, University of California San Diego, San Diego, California

[2]Department of Pharmacology, University of California San Diego, San Diego, California

[3]Department of Pathology, Moores Cancer Center, University of California San Diego, La Jolla, California

[4]Department of Surgery, Division of Surgical Oncology, University of California San Diego, San Diego, California

[5]Howard Hughes Medical Institute, University of California San Diego, San Diego, California

Abstract

Background and Objectives—Molecularly targeted fluorescent molecules may help detect tumors that are unseen by traditional white-light surgical techniques. We sought to evaluate a fluorescent ratiometric activatable cell penetrating peptide (RACPP) for tumor detection in a transgenic model of PTC.

Methods—Thirteen BRAFV600E mice with PTC were studied—seven injected intravenously with RACPP, four controls with saline. Total thyroidectomy was performed with microscopic white-light visualization. Fluorescent imaging of post-thyroidectomy fields was performed, and tissue with increased signal was removed and evaluated for PTC. Final samples were analyzed by a pathologist blinded to conditions. Vocal cord function was evaluated postoperatively with video laryngoscopy.

Results—The average in situ ratiometric (Cy5/Cy7) thyroid tumor-to-background contrast ratio was 2.27 +/−0.91. Fluorescence-guided clean-up following thyroidectomy identified additional tumor in 2 of 7 RACPP animals (smallest dimension 1.2 mm), and decreased the number of animals with residual tumor from 4 to 3. All retained tumor foci on final pathology were smaller than 0.76 mm. Intact vocal abduction was present in all of the RACPP animals.

*Correspondence to: Quyen T. Nguyen, MD, PhD, Department of Surgery, Division of Head and Neck Surgery, University of California San Diego, 9500 Gilman Drive La Jolla, San Diego, CA 92093-0647. Fax: 858-534-5270. q1nguyen@ucsd.edu.

Conflicts of interest: QTN and RYT: Scientific advisor to Avelas Biosciences which has licensed the ACPP technology from UCSD. There are no additional conflicts of interest.

Conclusions—RACPPs successfully targeted PTC in a transgenic thyroidectomy model, and allowed for residual tumor detection that reduced positive margins beyond what was possible with white-light surgery alone.

Keywords

surgical molecular guidance; activatable cell penetrating peptide; papillary thyroid cancer; BRAF V600E; murine model; laryngoscopy

INTRODUCTION

Our group has focused efforts on molecular targeting of cancer cells using activatable cell-penetrating peptides (ACPPs), which can be used for molecular imaging, drug delivery, and surgical guidance. Animal model work with ACPPs has demonstrated improved detection of tumors [1–3], and fluorescently labeled ACPPs have improved tumor resection [2], and disease-free survival [4,5].

Due to the availability of molecularly targeted radioactive iodine (RAI), microscopically clear surgical margins are not as absolute of a surgical necessity for papillary thyroid carcinoma (PTC) as they are in other solid tumors. Following total thyroidectomy RAI can be used as thyroid remnant ablation, adjuvant therapy, or treatment of known persistent disease [6]. Unfortunately, up to half of metastatic thyroid cancers will lose iodine concentrating ability and become RAI-refractory [7]. BRAF mutations are highly correlated with RAI-refractory metastatic PTC [8,9]. There is a need for novel molecular targeting techniques for PTC, particularly in aggressive cases with BRAF mutations, and those that are RAI-refractory.

To date, ACPP technology has not been utilized for molecular targeting of PTC. The ratiometric ACPP (RACPP) used in this study undergoes enzymatic activation by matrix metalloproteinases-2 and -9 (MMP-2,-9). There is evidence that MMP9 plays an important role in PTC progression and infiltration [10]. By utilizing MMP for molecular targeting and activation, the ACPP used in this study circumvents the necessity for RAI-avidity.

We used a $BRAF^{V600E}$ transgenic murine model to demonstrate iodine-independent molecular targeting of aggressive PTC using a fluorescently labeled RACPP for surgical molecular guidance. This is a clinically-relevant model for aggressive carcinoma because it leads to a phenotype that is histologically similar to humans with $BRAF^{V600E}$ PTC [11]. We hypothesized that molecular targeting of PTC could be achieved with this RACPP, and would increase the detection of tumor cells beyond what was possible using traditional white-light surgical techniques alone.

MATERIALS AND METHODS

Activatable Cell-Penetrating Peptides

The RACPP used in this study was synthesized as previously described [12,13] as a poly-arginine (poly-cationic) CPP moiety linked to a neutralizing poly-anionic tail via a linker that is cleaved by MMP-2 and MMP-9. The RACPP structure used in this study was: Cy7-

NH-e_9-c(peg_{12})oPLGC(Me)AG-r_9-c(Cy5) (previously referred to as RACPP PLGC(Me)AG) [13].

$BRAF^{V600E}$ Transgenic Murine Model of Papillary Thyroid Cancer

All animal procedures were approved by the University of California San Diego Institutional Animal Care and Use Committee and institutional review committee (IRB). A transgenic $BRAF^{V600E}$ murine model for spontaneous thyroid cancer was obtained in cooperation with the group that has previously described this model [11]. Animals with the $BRAF^{V600E}$ mutation develop hyperplastic goiter replaced by invasive PTC with tall-cell features. The animals were verified to be transgenic for $BRAF^{V600E}$ by genotyping tail tissue. Animals were allowed to mature in order to ensure a malignant phenotype, which was verified histologically as PTC infiltrating the entire thyroid gland.

Ratiometric Labeling of Thyroid Tumors

Following intraperitoneal injection of ketamine (50 mg/kg) and xylazine (1 mg/kg), 50 μl [10 nanomoles] of RACPP in saline was administered via retro-orbital injection. Saline was used as the injection in control animals. Two hours elapsed as a wash-out period prior to surgery.

Operative Procedures

White-light thyroidectomy—All animals underwent surgical excision of their thyroid cancer under white-light illumination. General anesthesia with inhalational isoflurane was adjusted to maintain robust respiration. With the animal in supine position, a midline skin incision was made from the submandibular region to the sternal notch. Underlying glandular tissue was separated and the strap muscles were retracted laterally. Using an operating microscope and micro-instruments, the thyroid isthmus was divided and left and right lobes were gently dissected laterally until each recurrent laryngeal nerve (RLN) was identified. Dissection proceeded from inferior to superior, with meticulous care taken to avoid damage to the RLNs. Handheld cautery was used sparingly at the superior vascular pedicle. Surgical time was recorded starting when the strap muscles were retracted, and ending upon completion of the cancer resection or fluorescent clean-up step, when applicable. The same surgeon performed all surgical procedures (RKO).

Fluorescence-guided clean-up—Following cancer resection under white-light, the surgical beds of RACPP animals were visualized with ratiometric fluorescence imaging using a customized dissecting microscope (Olympus MVX10 fluorescence ratio imaging system). The imaging parameters used in this study differed from prior work with ACPPs. In contrast to previous studies that used static fluorescence images, this study used real-time imaging in the living animal which relies on shorter exposure times (67–100 msec vs. 5,000 msec [12]). Additionally, this study used two narrow-band filters for real-time imaging on an operating microscope instead of full-spectrum, snapshot images. The fluorescence imaging parameters were optimized for each animal. Any tissue having an increased ratiometric signal ([tumor tissue Cy5/Cy7]/[adjacent background tissue Cy5/Cy7]) was deemed suspicious for tumor and removed for histological review.

Assessment of Laryngeal Function

Pre-operative laryngoscopy was performed 2 hr after injection. General anesthesia with inhalational isoflurane was adjusted to maintain a robust respiratory pattern. With the animal in the supine position, the tongue was retracted ventrally. A 2.3 mm endoscope was used to visualize the glottis. Spontaneous respiratory vocal fold motion was captured with high-definition video. The pre-operative assessment was a baseline to verify intact vocal function prior to the surgical procedures.

Repeat post-operative laryngoscopy was performed with video recording to evaluate RLN function immediately following thyroidectomy (or fluorescence-guided clean-up in RACPP animals). All videos underwent blinded reviewed by a laryngologist (PAW) to assess vocal fold mobility. Scoring was graded on a 3 point scale based on visualized maximal vocal fold movement (0 = immobile vocal fold, 1 = only twitching/dense paresis, 2 = incomplete movement/mild-moderate paresis, 3 = normal movement).

Final Margin Evaluation for Retained Thyroid Cancer

Following completion of thyroidectomy and fluorescence-guided clean-up, the animals were sacrificed. Tissue samples consisting of surgical bed quadrants (four samples per animal) were taken and analyzed for retained cancer. The presence of PTC in these final pathology specimens qualified as a positive surgical margin (margin evaluation phase).

Tissue samples were fixed in OCT, stained with hematoxylin and eosin (H&E), and reviewed by a pathologist blinded to experimental conditions. All tumor foci identified were measured with electronic calipers by the pathologist.

Fluorescence Imaging Analysis

Fluorescent images (Cy5 and Cy7) taken during fluorescence-guided clean-up were analyzed using ImageJ software. Areas representing thyroid tissue and adjacent non-thyroid tissue were hand-selected using the region-of-interest tool and the corresponding fluorescence intensities (Cy5 and Cy7) were calculated. Fluorescence contrast ratios referred to throughout the manuscript are ratiometric contrast values ([tumor tissue Cy5/Cy7]/[adjacent background tissue Cy5/Cy7]).

RESULTS

Thirteen transgenic $BRAF^{V600E}$ animals were available for this study. There were 11 complete surgeries with data for analysis—four control animals and seven RACPP animals. Two mortalities occurred prior to surgery secondary to over-sedation. The thyroid from one was dissected and images used for illustrative purposes (Fig. 1 displays the identification of PTC with RACPP). In the RACPP group, one animal died from iatrogenic carotid injury at the end of the thyroidectomy procedure.

The fluorescent clean-up phase did not significantly add to the duration of surgery—average operative time was 14 ± 3.5 min for controls versus 18 ± 5.4 min for the RACPP group ($P = 0.2$). A summary of surgical parameters and histological outcomes are provided in Table I.

Fluorescent Labeling of In Situ PTC Tumors

The in situ thyroid tumors from two RACPP animals were examined in order to confirm fluorescence uptake. The average ratiometric fluorescence contrast ratio of in situ thyroid tumors was 2.27 ± 0.91 (n = 2 animals, 4 thyroid lobes). The ratiometric image of the in situ thyroid tumor from one animal is shown in Figure 1. The highest signal is seen in the superior pole of the left thyroid lobe a ratiometric contrast value of 11.69 (asterisk).

Histological review of the thyroid tumor specimens revealed diffuse PTC. The PTCs were composed of cuboidal to columnar cells, clear and finely granular nuclei with grooves and multiple micronucleoli. The cells were arranged in various solid, diffuse, and micronodular patterns over a fibrotic stroma.

Intact Vocal Fold Function Following Fluorescence-Guided Clean-Up

Complete pre- and post-operative video laryngoscopy data was available for six RACPP animals. All post-operative vocal folds showed residual effect of anesthesia making movement sporadic. Intact vocal abductor motion was present in all of the RACPP animal vocal folds. A representative example of the visualization of the mouse larynx is provided in Figure 2. The endoscopic picture and video showed excellent resolution and anatomical detail.

Post-Thyroidectomy Fluorescence-Guided Clean-Up Identifies Residual Tumor Foci

Seven suspicious tissue areas were identified with fluorescence-guided clean-up. These seven signals were seen in the surgical beds of five of the seven RACPP animals (71.4% of animals, Table I). The lack of any fluorescent signal in control animals that did not receive RACPP injection was confirmed.

Two of the seven clean-up samples were histologically positive for PTC—Mouse H with a 1.2 mm tumor focus (contrast ratio 9.71, Fig. 3A and B) and Mouse I with a 3.3 mm focus (contrast ratio 1.52, Table I). Tissue samples from two animals were non-tumor, consisting of connective tissue, muscle, and adipose (Mouse F: contrast ratios 1.08, 1.29, and 1.32; and Mouse J: contrast ratio 1.20, Fig. 4A and C). One piece of tissue was too small for histological examination (Mouse K).

Final positive margins were seen in five of the twenty-eight quadrant samples from the seven RACPP animals (17.9% of the final thyroid bed quadrants). One of the four saline control animals (Mouse C) had retained tumor tissue on final pathology (6.3% of the sixteen post-surgical thyroid bed quadrants; tumor focus 0.01 mm).

Fluorescent RACPP positively identified two foci of residual PTC following white-light thyroidectomy, and decreased the number of animals with retained tumor from 4 to 3. In the three animals with final positive margins, the residual tumor foci were all less than 0.76 mm in greatest diameter (average 0.35 ± 0.30 mm, N = 5, Table I).

DISCUSSION

This is a proof-of-concept study demonstrating molecular targeting of PTC that is independent of iodine avidity. The fluorescently labeled RACPP used in this study has the ability to enhance detection of PTC beyond what is possible with white-light visualization alone. This model allowed for detection of residual microscopic cancer foci as small as 1.2 mm. The largest nest of residual cancer cells during the margin evaluation phase was 0.76 mm. Therefore, the size threshold for cancer detection for this current surgical model likely lies somewhere between 0.8 and 1.2 mm.

Based upon the fluorescence ratios reported in Table I, the fluorescence contrast ratio threshold used to detect true-positive cancer foci appears to be above 1.30. This is consistent with previously reported ratiometric threshold of 1.2 for the detection of cervical lymph node metastatases [12].

The imaging parameters and devices used in this study were optimized for real-time, in vivo imaging to simulate the surgical setting for future clinical translation. Short exposure times increase data noise and may reduce sensitivity. These imaging parameter considerations may partially explain the larger size threshold for tumor detection in the current study compared to our previous work [12]. Additionally, tumor foci detected on fluorescence-guided clean-up may have artificially low contrast ratios because small foci of cancer cells (high Cy5 signal, high contrast ratio) can be obscured by overlying normal tissue (low Cy5 signal, low contrast ratio). This may contribute to the false-negatives, and could also explain why the in situ contrast (2.27 ± 0.91) was higher than the contrast values of the small tumor foci detected during fluorescent clean-up. Future studies will be aimed at improving the surgical fluorescence-imaging equipment and parameters in order to optimize visualization and lower the size threshold of tumor detection.

Pathologic examination of human tumor specimens is typically done by sampling of the specimen at 2–4 mm intervals [14], and residual cancer in the surgical bed <1 mm may be missed. We do not know the true rate at which microscopic positive margins occur in patients with PTC; but fortunately, these lesions are probably ablated with post-surgical radioactive iodine in most cases. The largest piece of tumor removed in the fluorescence-guided clean-up phase can be classified as a macrometastasis (3.33 mm). The tumor foci that were left following surgery would be classified as micrometastases (largest 0.76 mm), or isolated tumor cells [15], and would fall below the detection threshold of current imaging modalities (ultrasound, PET/CT, MRI, scintigraphy).

Surgical time was not affected by the added use of intra-operative fluorescence guidance; and there was no compromise of post-thyroidectomy vocal cord function, although the study was not powered to show such differences. We developed a protocol for endoscopic laryngoscopy under anesthesia that allowed for the grading of vocal fold function following murine thyroidectomy. Endoscopic visualization of mouse larynges has been described in a vocal fold injury model [16], but to our knowledge, evaluation of murine vocal fold function has not been previously reported.

Papillary thyroid carcinoma carries a wide range of prognoses, ranging from excellent to poor, depending on metastasis, degree of differentiation, patient age, and RAI-avidity. Survival in well-differentiated PTC can be >95% at 5 years [17]. Conversely, patients with RAI-refractory cancers have limited treatment options. In cases of metastatic PTC, the 10 year survival rate is 92% in patients who achieve remission with RAI treatment, but drops to 29% in those who do not achieve remission, and is only 10% in patients with non-RAI avid tumors [18]. Treatment for RAI-resistant thyroid tumors is mostly limited to kinase inhibitors like sorafenib [19], or other targeted agents and clinical trials [20–22].

$BRAF^{V600E}$-positive PTC has been identified as a marker for aggressive subtype associated with advanced stage, tumor size and invasion, nodal involvement, recurrence, and absence of RAI avidity [9,23–29]. Mutations in $BRAF^{V600E}$ have been associated with non-radioiodine-avid status in patients with metastatic PTC [9]. Mutational testing for $BRAF^{V600E}$ can be used in humans to identify PTC patients at higher risk for more aggressive disease [30].

This study has several shortcomings that should be considered in the context of this model and possible extrapolations to other scenarios. The human correlate for positive margins in thyroid cancer is not as straightforward as with other tumors where recurrence and survival are strongly linked to positive surgical margins. Conversely, following thyroidectomy for high-risk PTC, radioactive iodine is used to ablate remaining thyroid tissue [6], decreasing the absolute necessity for negative margins. This study was not powered to compare the rates of persistent tumor cells, but previous ACPP work with another models demonstrated a favorable difference [2]. The surgical procedure of murine thyroidectomy is technically challenging, and it proved too difficult to conduct a long-term survival study, so we were unable to assess the clinical impact of retained PTC tissue. Notably, the surgeon was not blinded to the experimental condition which could introduce a bias toward aggressiveness of surgery.

CONCLUSIONS

RACPPs for fluorescence-guided surgery are a promising tool with potential to significantly impact future oncologic surgical practices. The molecular targeting of PTC demonstrated in this proof-of-concept study is a promising modality that may have applicability, particularly in cases of aggressive PTC that loses its RAI-avidity. Leveraging this iodine-independent molecular targeting for delivery of imaging or chemotherapeutic agents remains an exciting potential that warrants further investigation.

Acknowledgments

Grant sponsor: Burroughs-Wellcome Fund (CAMS); Grant sponsor: NIH R01; Grant numbers: EB014929-01, CA158448; Grant sponsor: NIH T32 Institutional Research Training; Grant number: DC000128; Grant sponsor: National Research Service Award (NRSA); Grant sponsor: Institutional Research Training; Grant numbers: T32 DC000128, 1R01CA158448-01A1, R01 EB014929-01.

This work was supported by a National Institutes of Health Ruth Kirschstein National Research Service Award (NRSA) Institutional Research Training Grant (T32 DC000128) to RKO, 1R01CA158448-01A1 to RYT; R01 EB014929-01 and Burroughs Wellcome Fund (CAMS) to QTN. The authors would like to thank Perla Arcaira for assistance with animal husbandry, and Nadia Nashi and Paul Steinbach for assistance with surgical procedures.

References

1. Jiang T, Olson ES, Nguyen QT, et al. Tumor imaging by means of proteolytic activation of cell-penetrating peptides. Proc Natl Acad Sci USA. 2004; 101:17867–17872. [PubMed: 15601762]
2. Nguyen QT, Olson ES, Aguilera TA, et al. Surgery with molecular fluorescence imaging using activatable cell-penetrating peptides decreases residual cancer and improves survival. Proc Natl Acad Sci USA. 2010; 107:4317–4322. [PubMed: 20160097]
3. Olson ES, Aguilera TA, Jiang T, et al. In vivo characterization of activatable cell penetrating peptides for targeting protease activity in cancer. Integr Biol (Camb). 2009; 1:382–393. [PubMed: 20023745]
4. Hussain T, Savariar EN, Diaz-Perez JA, et al. Surgical molecular navigation with ratiometric activatable cell penetrating peptide for intraoperative identification and resection of small salivary gland cancers. Head Neck. 2014; Epub ahead of print. doi: 10.1002/hed.23946
5. Metildi CA, Felsen CN, Savariar EN, et al. Ratiometric activatable cell-penetrating peptides label pancreatic cancer, enabling fluorescence-guided surgery, which reduces metastases and recurrence in orthotopic mouse models. Ann Surg Oncol. 2015; 22:2082–2087. [PubMed: 25319581]
6. Cooper DS, Doherty GM, Haugen BR, et al. Revised American Thyroid Association management guidelines for patients with thyroid nodules and differentiated thyroid cancer. Thyroid. 2009; 19:1167–1214. [PubMed: 19860577]
7. Schlumberger M, Tubiana M, De Vathaire F, et al. Long-term results of treatment of 283 patients with lung and bone metastases from differentiated thyroid carcinoma. J Clin Endocrinol Metab. 1986; 63:960–967. [PubMed: 3745409]
8. Ricarte-Filho JC, Ryder M, Chitale DA, et al. Mutational profile of advanced primary and metastatic radioactive iodine-refractory thyroid cancers reveals distinct pathogenetic roles for BRAF, PIK3CA, and A KT1. Cancer Res. 2009; 69:4885–4893. [PubMed: 19487299]
9. Yang K, Wang H, Liang Z, et al. BRAFV600E mutation associated with non-radioiodine-avid status in distant metastatic papillary thyroid carcinoma. Clin Nucl Med. 2014; 39:675–679. [PubMed: 24978326]
10. Marecko I, Cvejic D, Selemetjev S, et al. Enhanced activation of matrix metalloproteinase-9 correlates with the degree of papillary thyroid carcinoma infiltration. Croat Med J. 2014; 55:128–137. [PubMed: 24778099]
11. Knauf JA, Ma X, Smith EP, et al. Targeted expression of BRAFV600E in thyroid cells of transgenic mice results in papillary thyroid cancers that undergo dedifferentiation. Cancer Res. 2005; 65:4238–4245. [PubMed: 15899815]
12. Savariar EN, Felsen CN, Nashi N, et al. Real-time in vivo molecular detection of primary tumors and metastases with ratiometric activatable cell-penetrating peptides. Cancer Res. 2013; 73:855–864. [PubMed: 23188503]
13. Whitney M, Savariar EN, Friedman B, et al. Ratiometric activatable cell-penetrating peptides provide rapid in vivo readout of thrombin activation. Angew Chem Int Ed Engl. 2013; 52:325–330. [PubMed: 23080482]
14. Hinni ML, Ferlito A, Brandwein-Gensler MS, et al. Surgical margins in head and neck cancer: A contemporary review. Head Neck. 2013; 35:1362–1370. [PubMed: 22941934]
15. Hermanek P, Hutter RV, Sobin LH, et al. International Union Against Cancer. Classification of isolated tumor cells and micro-metastasis. Cancer. 1999; 86:2668–2673. [PubMed: 10594862]
16. Yamashita M, Bless DM, Welham NV. Surgical method to create vocal fold injuries in mice. Ann Otol Rhinol Laryngol. 2009; 118:131–138. [PubMed: 19326764]
17. Sherman SI. Thyroid carcinoma. Lancet. 2003; 361:501–511. [PubMed: 12583960]
18. Durante C, Haddy N, Baudin E, et al. Long-term outcome of 444 patients with distant metastases from papillary and follicular thyroid carcinoma: Benefits and limits of radioiodine therapy. J Clin Endocrinol Metab. 2006; 91:2892–2899. [PubMed: 16684830]
19. Thomas L, Lai SY, Dong W, et al. Sorafenib in metastatic thyroid cancer: A systematic review. Oncologist. 2014; 19:251–258. [PubMed: 24563075]
20. Falchook GS, Millward M, Hong DS, et al. BRAF inhibitor dabrafenib in patients with metastatic BRAF-mutant thyroid cancer. Thyroid. 2015; 25:71–77. [PubMed: 25285888]

21. Dadu R, Shah K, Busaidy NL, et al. Efficacy and tolerability of vemurafenib in patients with BRAF(V600E) -positive papillary thyroid cancer: M.D. Anderson Cancer center off label experience. J Clin Endocrinol Metab. 2015; 100:E77–E81. [PubMed: 25353071]
22. Locati LD, Licitra L, Agate L, et al. Treatment of advanced thyroid cancer with axitinib: Phase 2 study with pharmacokinetic/pharmacodynamic and quality-of-life assessments. Cancer. 2014; 120:2694–2703. [PubMed: 24844950]
23. Frasca F, Nucera C, Pellegriti G, et al. BRAF(V600E) mutation and the biology of papillary thyroid cancer. Endocr Relat Cancer. 2008; 15:191–205. [PubMed: 18310287]
24. Lee JH, Lee ES, Kim YS. Clinicopathologic significance of BRAF V600E mutation in papillary carcinomas of the thyroid: A meta-analysis. Cancer. 2007; 110:38–46. [PubMed: 17520704]
25. Fernandez IJ, Piccin O, Sciascia S, et al. Clinical significance of BRAF mutation in thyroid papillary cancer. Otolaryngol Head Neck Surg. 2013; 148:919–925. [PubMed: 23482475]
26. Nikiforov YE, Erickson LA, Nikiforova MN, et al. Solid variant of papillary thyroid carcinoma: Incidence, clinical-pathologic characteristics, molecular analysis, and biologic behavior. Am J Surg Pathol. 2001; 25:1478–1484. [PubMed: 11717536]
27. Kim TH, Park YJ, Lim JA, et al. The association of the BRAF (V600E) mutation with prognostic factors and poor clinical outcome in papillary thyroid cancer: A meta-analysis. Cancer. 2012; 118:1764–1773. [PubMed: 21882184]
28. Xing M, Alzahrani AS, Carson KA, et al. Association between BRAF V600E mutation and mortality in patients with papillary thyroid cancer. JAMA. 2013; 309:1493–1501. [PubMed: 23571588]
29. Xing M, Westra WH, Tufano RP, et al. BRAF mutation predicts a poorer clinical prognosis for papillary thyroid cancer. J Clin Endocrinol Metab. 2005; 90:6373–6379. [PubMed: 16174717]
30. Xing M, Clark D, Guan H, et al. BRAF mutation testing of thyroid fine-needle aspiration biopsy specimens for preoperative risk stratification in papillary thyroid cancer. J Clin Oncol. 2009; 27:2977–2982. [PubMed: 19414674]

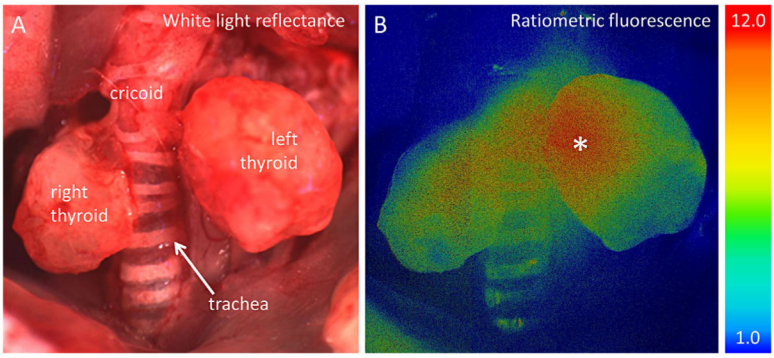

Fig. 1.

Identification of thyroid tumor with RACPPgr1. (**A**) White-light reflectance image of thyroid gland that is completely replaced by tumor and is enlarged (transgenic $BRAF^{V600E}$ mouse, Mouse L). The isthmus has been divided and left lobe dissected and retracted laterally to expose the tracheal rings. (**B**) Ratiometric fluorescence image showing that the tumor has an increased Cy5/Cy7 ratio, with a maximal contrast ratio of 11.69 in the central area of left lobe (*). Cy5/Cy7 ratiometric scale bar shows low ratio (blue) up to high ratio (red).

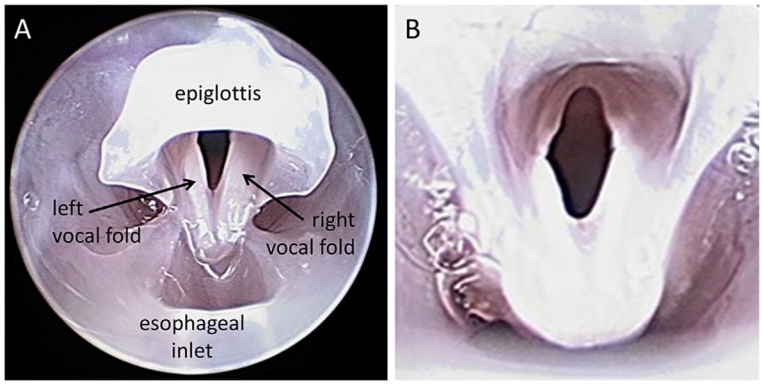

Fig. 2.

Endoscopic view of mouse larynx. (**A**) Endoscopic view of mouse larynx in the open position showing the excellent resolution and anatomical detail that can be seen with murine endoscopic video laryngoscopy. (**B**) Close-up view of the same glottis as in A.

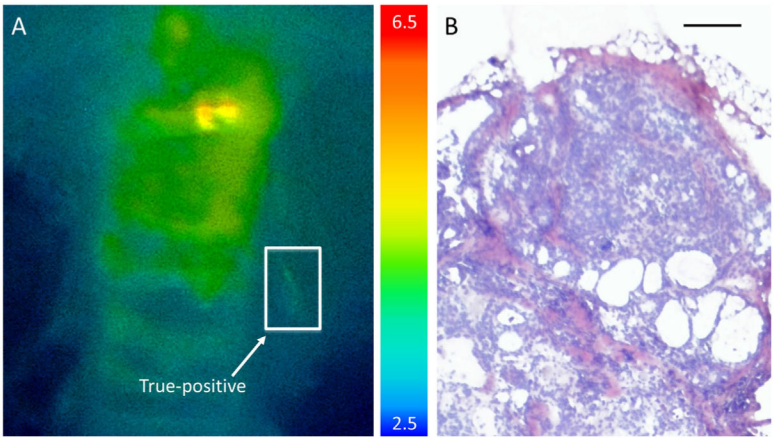

Fig. 3.

True-positive ratiometric fluorescent clean-up images with corresponding histology. (**A**) Ratiometric fluorescence image of the thyroid bed of transgenic $BRAF^{V600E}$ mouse (mouse I) following thyroidectomy with white-light visualization showing a small focus of fluorescent signal in the left inferior thyroid bed (yellow box, [Cy5/Cy7 specimen]/[Cy5/Cy7 background] ratio = 1.52) of transgenic $BRAF^{V600E}$ mouse following thyroidectomy with white-light visualization. No abnormal tissue was visible in this region using white-light visualization. This tissue was removed during fluorescence clean-up, and was a true-positive (i.e., papillary thyroid carcinoma identified). Cy5/Cy7 ratiometric scale bar shows low ratio (blue) up to high ratio (red). (**B**) Histology slide of 3.33 mm focus of papillary thyroid cancer that was removed during fluorescence-guided clean-up phase shown in A. Hematoxylin and eosin stain. Scale bar = 100 μm.

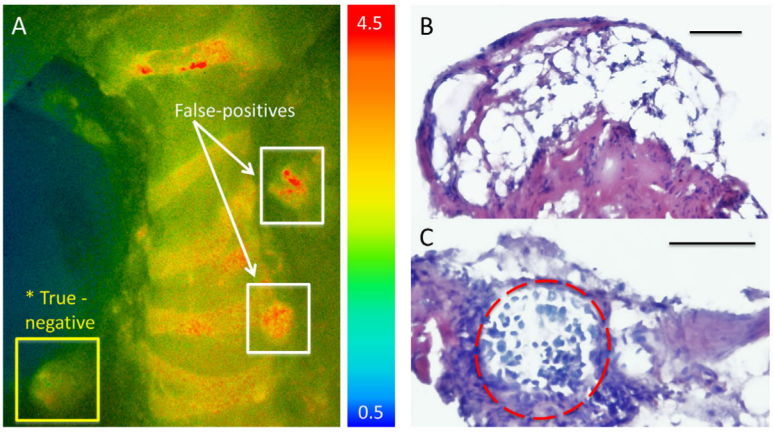

Fig. 4.

False-positive and true-negative ratiometric fluorescent clean-up images with corresponding histology. (**A**) Ratiometric fluorescence image of the thyroid bed of transgenic $BRAF^{V600E}$ mouse (mouse F) following thyroidectomy with white-light visualization showing three foci of tissue with increased fluorescent signal—two in the left thyroid bed (false-positives, white boxes ratio = 1.32 and 1.29) and one in the right inferior thyroid bed (true-negative, yellow box, ratio = 1.08). No abnormal tissue was visible in either region with white-light visualization. All three specimens were removed during fluorescence clean-up (note that the fluorescence ratio scale bar is lower compared to the true-positive Figure 3A in order to highlight the differences between specimen and adjacent background). Cy5/Cy7 ratiometric scale bar shows low ratio (blue) up to high ratio (red). There was no evidence of tumor in any of the three foci (see B). (**B**) Histology slide of false-positive (non-tumor) tissue seen in A. Hematoxylin and eosin stain. Scale bar = 100 μm. (**C**) On final margin evaluation of the surgical bed following fluorescence-guided cleanup, we identified a 100 um focus of papillary thyroid cancer (red dotted line). This samples was taken from the right inferior surgical bed quadrant, adjacent to the true-negative specimen (A, yellow box and *). Hematoxylin and eosin stain. Scale bar = 100 μm.

TABLE I

Surgical Data and Outcomes

	Surgical time, minutes (N)	Fluorescent signal following white-light thyroidectomy	Tissue components removed under fluorescence-guided clean-up	Retained papillary thyroid cancer on final pathology (positive quadrants; 4 quadrants evaluated per animal)
No RACPP (control animals)				
Overall	14(4)	n/a	n/a	1 of 16 (6.3%)
Mouse A	11	–	–	No
Mouse B	19	–	–	No
Mouse C	13	–	–	1 quadrant 0.01 mm tumor focus
Mouse D	13	–	–	No
RACPP (study animals)				
Overall	18 (7)	5 of 7 (71.4%)	2 of 7 (28.6%)	5 of 28 (17.9%)
Mouse E	26	No	None	No
Mouse F	18	Yes, right inferior pole (contrast ratio 1.08) and two left paratracheal (contrast ratios 1.32 and 1.29)	Connective tissue, muscle, adipose	1 quadrant 0.04 mm tumor focus
Mouse G	13	No	None	2 quadrants 0.04 mm and 0.32 mm tumor foci
Mouse H	20	Yes, left inferior quadrant (contrast ratio 9.71)	Tumor focus 1.2 mm	2 quadrants 0.54 mm and 0.76 mm tumor foci
Mouse I	10	Yes, left paratracheal (contrast ratio 1.52)	Tumor focus 3.3 mm	No
Mouse J	22	Yes, right carotid region (contrast ratio 1.20)	Connective tissue	No
Mouse K	17	Yes, left inferior pole (contrast ratio 1.18)	Tissue too small to process and review	No

Contrast ratios signify thyroid Cy5/Cy7/adjacent Cy5/Cy7 contrast.

All thyroid glands contained diffuse papillary thyroid carcinoma.